



OPEN

Calcium metaborate induced thin walled carbon nanotube syntheses from CO₂ by molten carbonate electrolysis

Xirui Wang, Xinye Liu, Gad Licht & Stuart Licht✉

An electrosynthesis is presented to transform the greenhouse gas CO₂ into an unusually thin walled, smaller diameter morphology of Carbon Nanotubes (CNTs). The transformation occurs at high yield and coulombic efficiency of the 4-electron CO₂ reduction in a molten carbonate electrolyte. The electrosynthesis is driven by an unexpected synergy between calcium and metaborate. In a pure molten lithium carbonate electrolyte, thicker walled CNTs (100–160 nm diameter) are synthesized during a 4 h CO₂ electrolysis at 0.1 A cm⁻². At this low current density, CO₂ without pre-concentration is directly absorbed by the air (direct air capture) to renew and sustain the carbonate electrolyte. The addition of 2 wt% Li₂O to the electrolyte produces thinner, highly uniform (50–80 nm diameter) walled CNTs, consisting of ~75 concentric, cylindrical graphene walls. The product is produced at high yield (the cathode product consists of >98% CNTs). It had previously been demonstrated that the addition of 5–10 wt% lithium metaborate to the lithium carbonate electrolyte boron dopes the CNTs increasing their electrical conductivity tenfold, and that the addition of calcium carbonate to a molten lithium carbonate supports the electrosynthesis of thinner walled CNTs, but at low yield (only ~15% of the product are CNTs). Here it is shown that the same electrolysis conditions, but with the addition of 7.7 wt% calcium metaborate to lithium carbonate, produces unusually thin walled CNTs uniform (22–42 nm diameter) CNTs consisting of ~25 concentric, cylindrical graphene walls at a high yield of >90% CNTs.

CO₂ is the most prominent of the greenhouse gases, and due to greenhouse gas increase the planet is heating up. Atmospheric CO₂ concentration, which had cycled at 235 ± ~50 ppm for 400 millennia until 1,850, is currently at 416 ppm and rising at a rapid annual rate incurring global planetary climate disruptions and habitat loss^{1–4}. CO₂ was regarded as such a stable molecule that its transformation into a non-greenhouse gas posed a major challenge⁵. Conventional methodologies of carbon nanomaterial production have a high carbon footprint. For example, Chemical Vapor Deposition, CVD, is an energy intensive, expensive process to produce carbon nanomaterial associated with an unusually massive carbon footprint of up to 600 tonnes of CO₂ emitted per tonne of carbon nanomaterial product⁶.

In 2009 and 2010 a novel sunlight driven methodology to split CO₂ into carbon and oxygen by molten carbonate electrolysis was introduced^{7,8}. This process does not require sunlight, and it was demonstrated that using a molten carbonate and a variety of electrolytic configurations, the carbon product can be made into pure carbon nanomaterials, such as Carbon Nanotubes (CNTs)^{9–24}. For example, this novel chemistry transforms the greenhouse Carbon dioxide to Carbon NanoTubes (C2CNT), and directly captures and CO₂ from the atmosphere or from concentrated anthropogenic CO₂ sources such as power plant exhaust. Several different carbon allotropes can be produced by C2CNT. This report focuses on the synthesis of thin walled CNTs from CO₂ by a modification of this methodology.

The C2CNT process, has quantified the high affinity of molten carbonates to absorb both atmospheric and flue gas levels of CO, Utilizing the ¹³C isotope of CO₂ to track in-flux, we have previously demonstrated in molten lithium carbonate that CO₂ originating from the gas phase serves as the renewable carbon building blocks in the observed CNT product^{10,11}. The net reaction is in accord with:

Department of Chemistry, George Washington University, Washington, DC 20052, USA. ✉email: slicht@gwu.edu

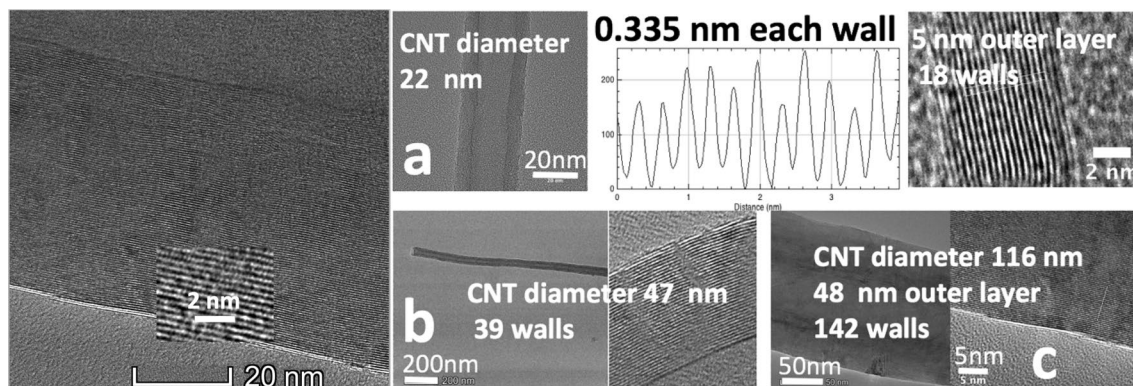


Figure 1. TEM of carbon nanotube walls in molten carbonated synthesized CNTs. The synthesis is by 0.2 (add space) A cm² electrolysis in 770 °C Li₂CO₃ at a 5 cm² coiled copper wire and Ni powder). Left: an expanded view of the CNT product after 90 min synthesis. The synthesis produces a pure CNT product whose diameter, and number of cylindrical graphene walls increases with electrolysis time. TEM of the synthesis product after **a**: 15, **b**: 30 or **c**: 90 min electrolysis.

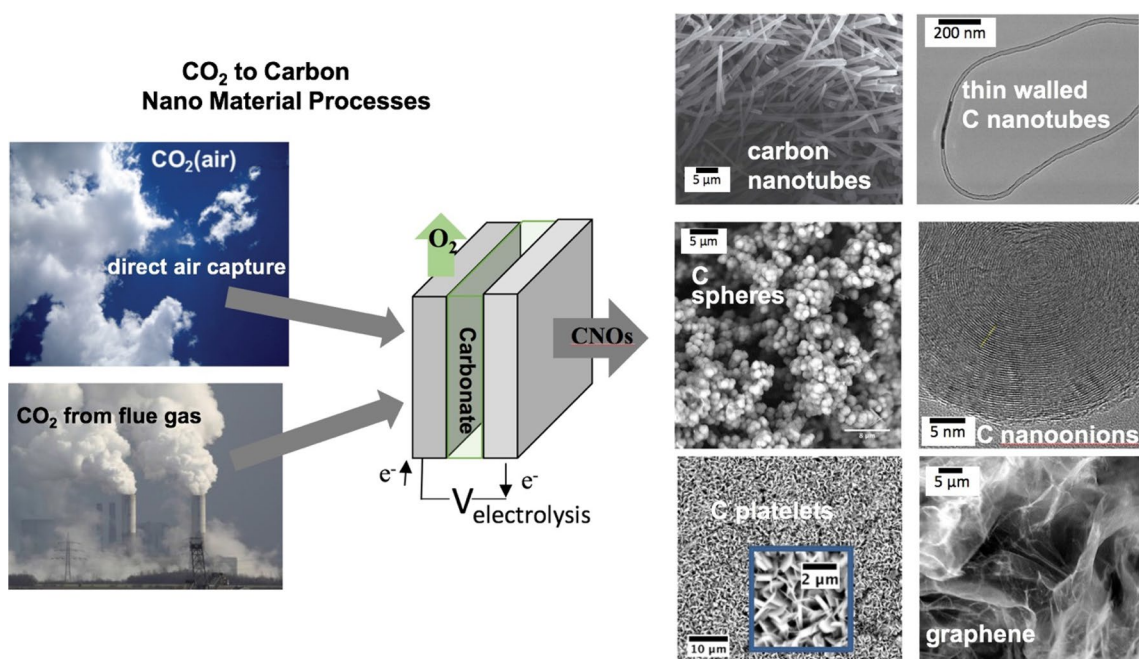
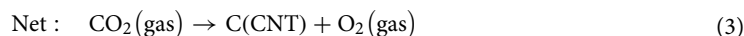
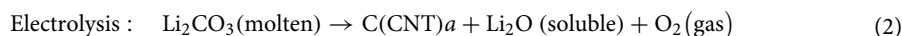
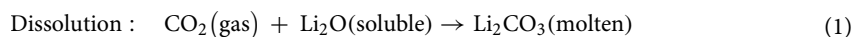


Figure 2. High yield electrolytic synthesis of carbon nanomaterials from CO₂, either directly from the air or from smokestack CO₂, in molten carbonate^{11,19,22,23}.



An important component of the C2CNT growth process is transition metal nucleated growth, such as the addition of nickel powder which leads to clearly observable CNT walls as shown in Fig. 1. However, when these nucleation additives are purposely excluded during the synthesis, then the high yield synthesis of carbon nanoions (spheres) (as shown in Fig. 2) or graphene are accomplished^{19,22}.

Many different carbon allotropes can be produced by molten CO₂ splitting also referred to as the Genesis Device™. The wide range of carbon nanomaterial morphologies observed shows the potential for tuning the product for uses in many different useful products. Here, we present synthesis of unusually thin walled CNTs,

which would have particular use in applications requiring less rigid CNTs; for example, for nano connections within circuits, and conductive pastes²⁵. Unlike previous methodologies to synthesize thin walled CNTs, this new methodology is inexpensive (using inexpensive materials and electrosynthesis) and is the only methodology which is carbon negative to help mitigate climate change. The synthesis finds an unexpected synergy by combining in a single step, a previous low yield but thin walled CNT electrosynthesis, and a boron doping CNT electrosynthesis. The new high yield product is significant both due to its morphology, and green carbon footprint as the methodology uses CO₂ as a reactant making it carbon negative.

Experimental

Experiment materials and procedure. Lithium carbonate (Li₂CO₃, 99.5%), lithium oxide (Li₂O, 99.5%), calcium oxide (CaO, 99.5%) and boric acid (H₃BO₃, 99.9%) are used as the electrolyte in this study.

Electrolysis and purification. The electrolyte is pre-mixed in the noted ratios. Unlike early studies, such as shown in Fig. 1, that used 1 cm separated, horizontally aligned anodes and cathodes disks comprised of coiled wires, this study uses electrodes that are sheet metal and vertically immersed into the molten salt electrolyte. 0.25-inch-thick Muntz brass sheet is used as the cathode, and 0.04-inch-thick Nichrome (chromel A) sheet is used as the anode. The cathode is aligned (sandwiched) between two series connected anodes, and the cathode is spaced 1 cm from each of the anodes. The electrolyte and electrodes are contained in a rectangular stainless steel 304 case. Unlike, the experiments described in Fig. 1 which was at a constant current of 0.2 A/cm² for different short intervals of time (15, 30 or 90 min), here, for the vertically immersed planar electrodes a constant current of 0.1 A/cm² is applied for a constant time of 4 h. The electrolysis temperature is 770 °C. The raw product is collected from the brass cathode after the experiment and cooled down, followed by an aqueous wash procedure. The washed carbon product is separated by vacuum filtration. The washed carbon product is dried overnight at 60 °C in an oven yielding a black power product.

The coulombic efficiency of electrolysis is the percent of applied, constant current charge that was converted to carbon determined as:

$$100\% \times C_{\text{experimental}}/C_{\text{theoretical}} \quad (4)$$

This is measured by the mass of washed carbon product removed from the cathode, $C_{\text{experimental}}$, and calculated from the theoretical mass, $C_{\text{theoretical}} = (Q/nF) \times (12.01 \text{ g C mol}^{-1})$ which is determined from Q , the time integrated charged passed during the electrolysis, F , the Faraday (96,485 As mol⁻¹ e⁻), and the $n = 4 \text{ e}^- \text{ mol}^{-1}$ reduction of tetravalent carbon.

Characterization. Samples are analyzed by PHENOM Pro Pro-X SEM, FEI Teneo LV SEM, and by FEI Teneo Talos F200X TEM.

Results and discussion

The electrolytic splitting of CO₂ in molten carbonate electrodes can be conducted with a wide range of cathode materials including iron, steels, nickel, nickel alloys, Monel, copper and brass. The diameter of the CNTs grown on copper or on brass cathodes tends to be similar. In Fig. 1, concentric CNT walls separated by 0.335 nm, which is typical of the distinctive one atom thick separation of multiple graphene layers are observed. Figure 1 demonstrates when the electrolyte is conducted in pure Li₂CO₃ an increase in CNT diameter from 22 to 116 nm occurs when the constant current electrolysis time is increased from 15 to 90 min. The CNT is composed of concentric, cylindrical graphene walls spaced 0.335 nm apart. Alongside the increased diameter is an increase in the number of concentric CNT walls on each of the inner sides of the nanotube increase from 18 to 142 graphene layers. In pure Li₂CO₃, for 4 h, rather than 1.5 h electrosynthesis, the CNT continues to grow, and on the average the CNT diameter ranges from 100 to 160 nm, for example with repeat a 4 h constant current electrolyses.

The electrolyte composition can affect the CNT diameter. Figure 3 presents SEM of the thinnest 4 h grown CNTs that had been observed. This is accomplished by addition of low concentrations of lithium oxide to the electrolyte. The CNTs are electrosynthesized in 770 °C Li₂CO₃ with 2 wt% Li₂O electrolyte (0.67 mol of Li₂O per kg Li₂CO₃) using a nickel alloy anode and brass cathode. At the relatively low current density of 0.1 A/cm² applied (aluminum smelting by electrolysis of aluminum oxide typically occurs at 0.5–0.6 A/cm²), CO₂ from the air (direct air capture) is sufficient to renew the electrolyte in accord with Eq. (3) and maintain the electrolyte level in accord with Eq. (1), and concentrated addition of CO₂ is not required and not added. Nickel chromium alloy anodes and brass cathodes have been shown to be particularly stable for repeated use in CO₂ splitting by molten carbonate electrolysis²¹. After the synthesis, the extracted cathode is cooled and the solid product readily is peeled off the cathode and washed to remove excess electrolyte prior to microscopy. Panel B of Fig. 3 is of interest as it constitutes SEM of a product removed from the rear side (not facing the anode) of the cathode. In particular, a piece of the multilayer graphene sheet which first forms on the cathode, and from which the CNTs growth is evident in a manner consistent with the tip growth mechanism presented in reference 3. The product is ~98% uniform CNTs as determined by visual inspection of multiple SEMs and TEM. Repeat experiments using the 2 wt% Li₂O in Li₂CO₃ electrolyte, the coulombic efficiency was consistently 97% to 100%. Lower concentrations of lithium oxide resulted in thicker diameter and CNTs, and greater than 2 wt% added lithium oxide did not further decrease the observed CNT product thickness. The diameter of representative samples of the CNTs was

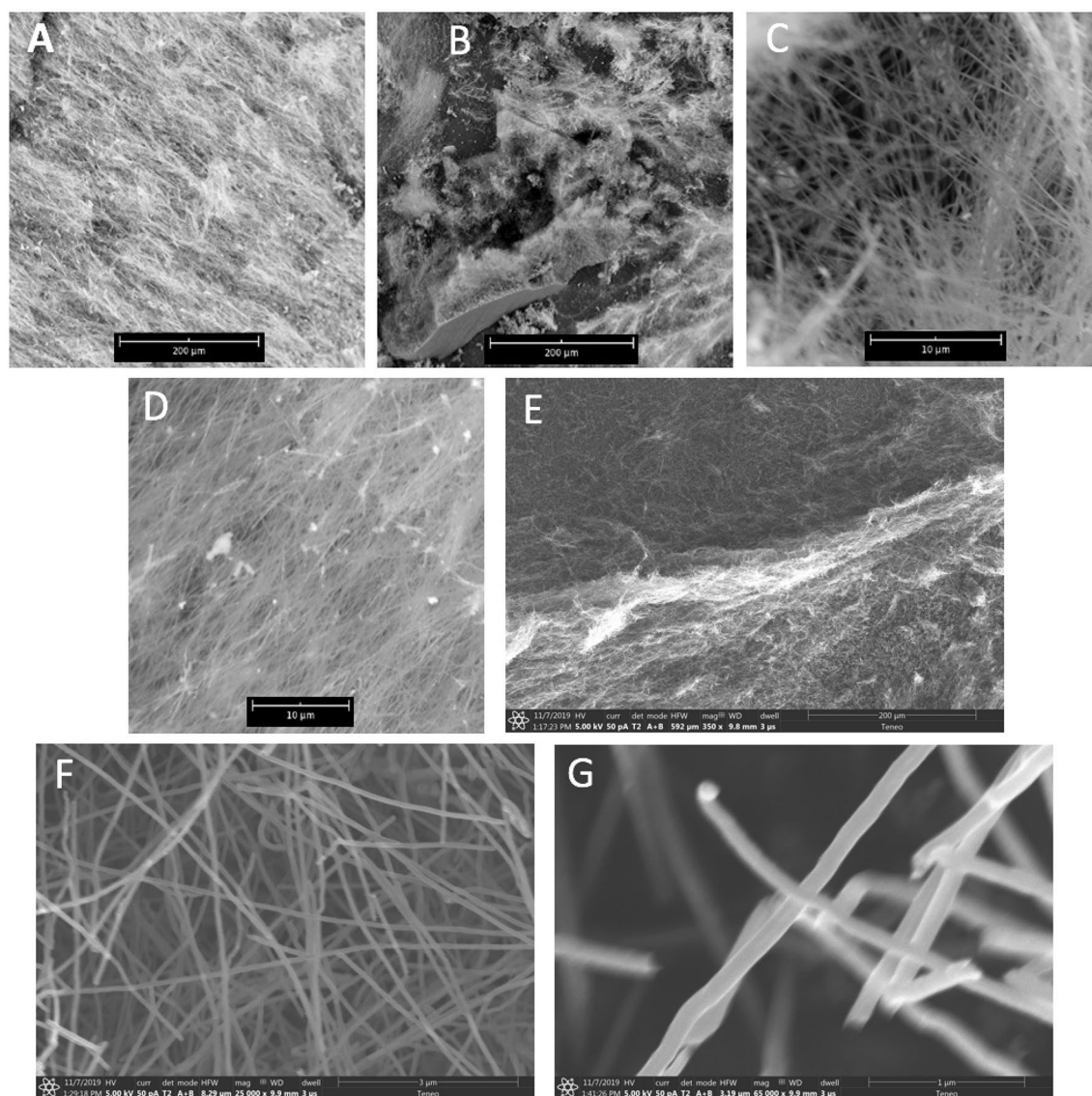


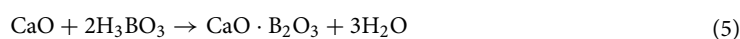
Figure 3. SEM (panels A–G) of the CNTs product of CO₂ splitting in a molten Li₂CO₃ electrolyte containing 0.67 molal (2 wt%) Li₂O. The scale bars in SEM (A–E) are respectively at 200, 200, 10, and 10 μm. The scale bars in TEM (E–G) are respectively at 200, 3 and 1 μm.

measured with the nano-caliper function of the Phenom SEM and varied from ~50 to 80 nm, or approximately half the diameter of CNTs electro synthesized in pure Li₂CO₃ without added Li₂O.

It had previously been demonstrated that the addition of 5–10 wt% LiBO₂ to a Li₂CO₃ electrolyte, used in CO₂ electrolysis, boron dopes the CNTs increasing their electrical conductivity tenfold¹⁸. It had also been shown the addition of alkali earth metal carbonates to a lithium electrolyte have a substantial effect on the carbon nanomaterial electrolysis product. For example, the addition of magnesium carbonate prevented the formation of CNTs, and the addition of CaCO₃ inhibited, and diminished, but allowed the formation of CNTs resulting in a yield of only ~15 CNT product¹⁵. Interestingly, it was observed that those CNTs which did form in the Ca/Li mixed carbonate electrolyte had much thinner walls than those synthesized in pure lithium carbonate¹⁵.

Of the metaborate salts, and their molten phase counterparts, sodium metaborate is that which is most studied, which is likely due to its use in certain formulations of glass^{26–30}. To a lesser extent calcium borate, CaB₂O₄ or CaO·B₂O₃, has also been studied^{31–33}. Note that the boron in calcium metaborate has a ratio Ca to B to O ratio of 1:2:4, whereas the ratio in calcium borate, common name Gersely borate, Ca₃(BO₃)₂ is 1:2/3:2.

Calcium metaborate in this study, was synthesized by the addition of calcium oxide and boric acid:



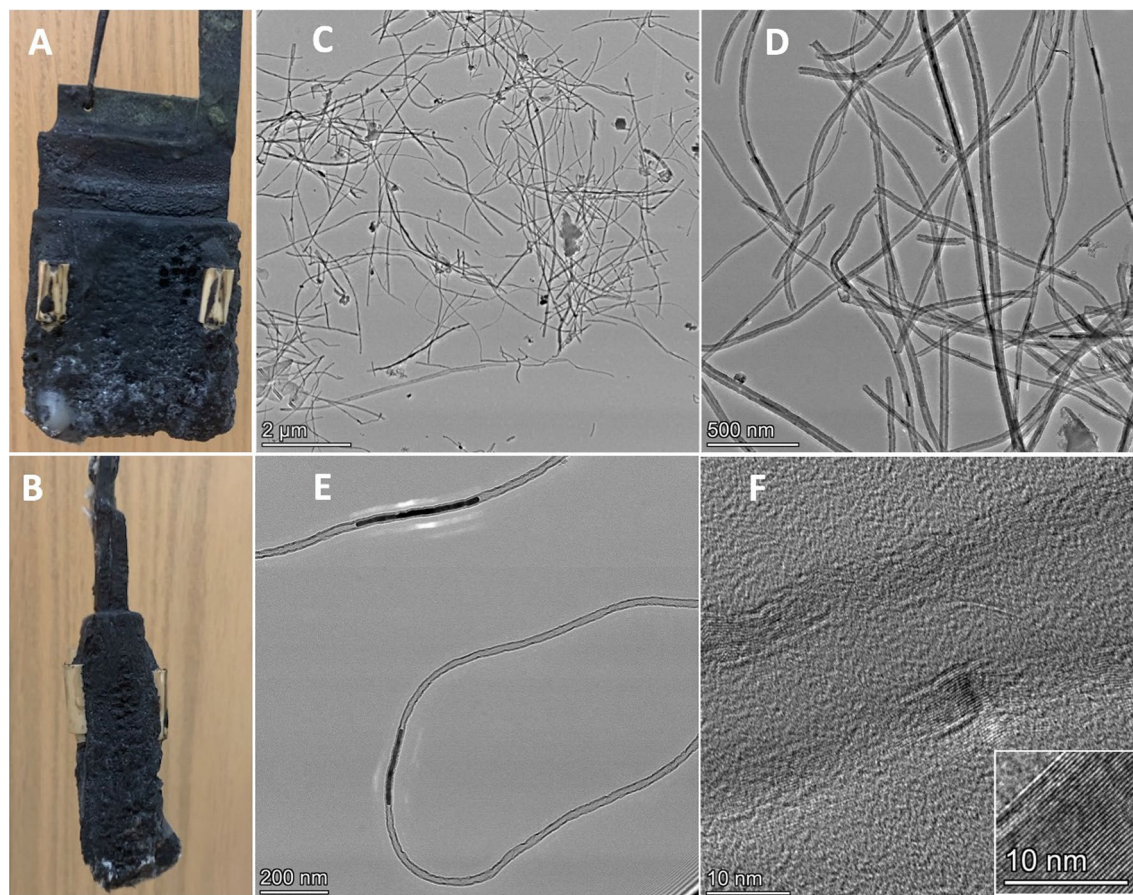


Figure 4. Photos of the extracted cathode (A,B) and TEM (of the CNT product) after CO₂ electrolytic splitting in a molten Li carbonate electrolyte containing 0.67 molal calcium metaborate. The scale bars in the TEM are respectively at 2 μm (C), 500 nm (D), 200 nm (E) and 10 nm (F).

Specifically, 0.2 mol of Ca and 0.4 mol of boric acid were added to 300 g Li₂CO₃ and heated at 770 °C overnight to release all water as steam. The electrolysis of CO₂ uses a molten electrolyte mix of 0.67 molal (7.7 wt%) CaO·B₂O₃ in Li₂CO₃, with a 6 cm by 7 cm brass cathode sandwiched between nichrome anodes. The electrolysis approaches 100% coulombic efficiency as measured according to Eq. (4), and the product consists of 2–6 μm length CNTs, and is marginally less pure (90% yield of CNTs) than the 0.67 molal Li₂O synthesis. The cathode is extracted and cooled, after a 4 h electrolysis is shown on the left side of Fig. 4. White cylinders in the photo are alumina placed on the cathode to prevent shorting with the anode. The graphitization of the thin walls is demonstrated in the inset of panel F by the individual carbon nanotubes which are flat and separated by 0.34 nm, which is the same as graphene layers in graphite¹¹.

The diameter of representative CNTs of the calcium borate in Li₂CO₃ electrosynthesized CNTs varied from ~22 to 42 nm which is considerably smaller than in similar pure lithium carbonate or lithium carbonate with lithium oxide electrolytes. The distribution of CNT diameter size by count is compared in Fig. 5 between the CNT product formed from Li₂CO₃ electrolyte, either containing 0.67 m Li₂O (top), or 0.67 m CaO·B₂O₃ (bottom). The average CNT diameter after a 4 h electrolysis is 130 nm in Li₂CO₃ without additives, 65 nm with 0.67 m Li₂O and 32 nm with 0.67 m CaO·B₂O₃.

Conclusions

We present a new high yield pathway to produce thin walled carbon nanotubes. The process uses a calcium metaborate dissolved in a molten Li₂CO₃ electrolyte, and splits and consumes CO₂ as the carbon source building blocks of the carbon nanotubes. Using equivalent 4 h CO₂ 770 °C electrolyses at 0.1 A cm⁻², the carbon CNT products of electrolyses in a pure molten lithium carbonate electrolyte, have a diameter of 100 to 160 nm. Those conducted in lithium carbonate containing 0.67 m Li₂O have a diameter of 50 to 80 nm, while those containing 0.67 m CaO·B₂O₃ have a diameter of 22–42 nm diameter. Each range of carbon nanotube morphology has various applications in energy storage, high strength composites, conductive pastes and as catalysts.

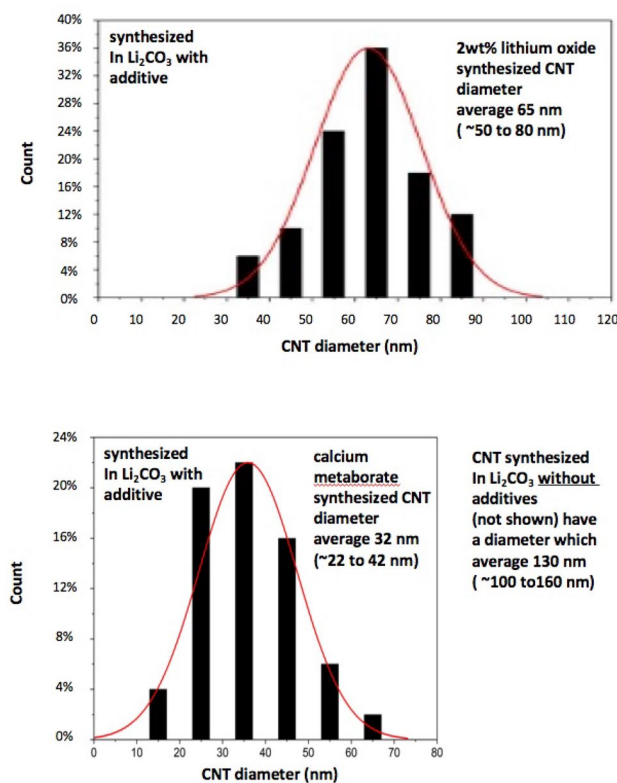


Figure 5. The distribution of CNT diameter size by count is compared between the CNT product formed on lithium carbonate electrolyte, either containing 0.67 m Li_2O (top), or 0.67 m $\text{CaO}\cdot\text{B}_2\text{O}_3$ (bottom). After the same electrolysis, but in a pure Li_2CO_3 electrolyte (without additives), the average CNT diameter after a 4 h electrolysis is ~130 to 160 nm.

In accord with Fig. 1, it is likely that the diameter may be decreased approximately eightfold by a 15 min, rather than 4 h electrolysis. In a similar manner, electrolyses conducted for the same period, but with a lower current density will likely also exhibit fewer CNT walls and smaller CNT diameters. The high yield, high coulombic efficiency molten carbonate electro-synthesis of single and double walled CNTs may be within reach and achieved by combining appropriate electrolyte additives, such as calcium metaborate, with low current density and short electrolysis times.

Received: 10 May 2020; Accepted: 17 August 2020

Published online: 15 September 2020

References

- CO₂-earth. Daily CO₂ Values. *CO₂-earths*, <https://www.co2.earth/daily-co2> (2020).
- NASA: Global Climate Change. Global Climate Change: The Relentless Rise of Carbon Dioxide. NASA: Global Climate Change. NASA, https://climate.nasa.gov/climate_resources/24/ (2017).
- Urban, M. C. Accelerating extinction risk from climate change. *Science* **348**, 571–573 (2015).
- Pimm, S. L. Climate disruption and biodiversity. *Curr. Biol.* **19**, R595–R601 (2009).
- Praksh, G.K., Olah, G.A., Licht, S. & Jackson, N. B. Reversing Global Warming: Chemical Recycling and Utilization of CO₂, *Report of 2008 NSF Workshop*. <https://loker.usc.edu/ReversingGlobalWarming.pdf> (2008).
- Khanna, V., Bakshi, B. R. & Lee, L. J. Carbon nanofiber production: Life cycle energy consumption and environmental impact. *J. Ind. Ecol.* **12**, 394–410 (2008).
- Licht, S. STEP (solar thermal electrochemical photo) generation of energetic molecules: a solar chemical process to end anthropogenic global warming. *J. Phys. Chem. C* **113**, 16283–16292 (2009).
- Licht, S. *et al.* New solar carbon capture process: STEP carbon capture. *J. Phys. Chem. Lett.* **1**, 2363–2368 (2010).
- Ren, J., Li, F., Lau, J., Gonzalez-Urbina, L. & Licht, S. One-pot synthesis of carbon nanofibers from CO₂. *Nano Lett.* **15**, 6142–6148 (2015).
- Ren, J., Lau, J., Lefler, M. & Licht, S. The minimum electrolytic energy needed to convert carbon dioxide to carbon by electrolysis in carbonate melts. *J. Phys. Chem. C* **119**, 23342–23349 (2015).
- Ren, J. & Licht, S. Tracking airborne CO₂ mitigation and low cost transformation into valuable carbon nanotubes. *Sci. Rep.* **6**, 27760–27761–11 (2016).
- Licht, S. *et al.* Carbon nanotubes produced from ambient carbon dioxide for environmentally sustainable lithium-ion and sodium-ion battery anodes. *ACS Cent. Sci.* **2**, 162–168 (2016).
- Lau, J., Dey, G. & Licht, S. Thermodynamic assessment of CO₂ to carbon nanofiber transformation for carbon sequestration in a combined cycle gas or a coal power plant. *Energy Conser. Manag.* **122**, 400–410 (2016).

14. Dey, G., Ren, J., El-Ghazawi, O. & Licht, S. How does an amalgamated Ni cathode affect carbon nanotube growth?. *RSC Adv.* **122**, 400–410 (2016).
15. Ren, J., Johnson, M., Singhal, R. & Licht, S. Transformation of the greenhouse gas CO₂ by molten electrolysis into a wide controlled selection of carbon nanotubes. *J. CO₂ Util.* **18**, 335–344 (2017).
16. Licht, S. Co-production of cement and carbon nanotubes with a carbon negative footprint. *J. CO₂ Util.* **18**, 378–389 (2017).
17. Johnson, M. *et al.* Data on SEM, TEM and Raman spectra of doped, and wool carbon nanotubes made directly from CO₂ by molten electrolysis. *Data Br.* **14**, 592–606 (2017).
18. Johnson, M. *et al.* Carbon nanotube wools made directly from CO₂ by molten electrolysis: value driven pathways to carbon dioxide greenhouse gas mitigation. *Mater. Today Energy* **5**, 230–236 (2017).
19. Liu, X., Ren, J., Licht, G., Wang, X. & Licht, S. Carbon nano-onions made directly from CO₂ by molten electrolysis for greenhouse gas mitigation. *Adv. Sustain. Syst.* **1900056**, 1–10 (2019).
20. Licht, S. *et al.* Amplified CO₂ reduction of greenhouse gas emissions with C2CNT carbon nanotube composites. *Mater. Today Sustain.* **6**, 100023 (2019).
21. Wang, X., Liu, X., Licht, G., Wang, B. & Licht, S. Exploration of alkali cation variation on the synthesis of carbon nanotubes by electrolysis of CO₂ in molten carbonates. *J. CO₂ Util.* **18**, 303–312 (2019).
22. Ren, J. *et al.* Recent advances in solar thermal electrochemical process (STEP) for carbon neutral products and high value nano-carbons. *Accounts Chem. Res.* **52**, 3177–3187 (2019).
23. Liu, X., Wang, X., Licht, G., & Licht, S. Transformation of the greenhouse gas carbon dioxide to graphene. *J. CO₂ Util.*, **36**, 288–294 (2020).
24. Wang, X., Sharif, F., Liu, X., Licht, G., Lefler, M., & Licht, S. Magnetic carbon nanotubes: Carbide nucleated electrochemical growth of ferromagnetic CNTs from CO₂. *J. CO₂ Util.* **40**, 101218 1–10 (2020).
25. Cheaptubes.com. Thin Walled Carbon Nanotubes., *Single Walled Carbon Nanotubes*, <https://www.cheaptubes.com/product/thin-walled-carbon-nanotubes> (2020).
26. Boddanov, V. N., Mikhailov, I. G. & Nemilov, S. V. *Phys. Chem. Glasses. Sov. Phys. Acoust.* **20**, 310–313 (1975).
27. Sato, M. & Yokokawa, T. Concentration overpotential of Pt-oxygen electrode reaction in molten Na₂O–B₂O₃. *Trans. JIM* **16**, 441–444 (1975).
28. Itoh, H., Sasahira, A., Makeawa, T., & Yokokawa, T. Electromotive-force measurements of molten oxide mixtures. Part 8—thermodynamic properties of Na₂O–B₂O₃ melts. *J. Chem. Soc. Faraday Trans. 1* **80**, 473–487 (1984).
29. Claes, P., Coq, J. L. & Glibert, J. Electrical conductivity of molten B₂O₃–Na₂O mixtures. *Electrochim. Acta* **33**, 347–352 (1988).
30. Park, S. & Sohn, I. Effect of Na₂O on the high-temperature thermal conductivity and structure of Na₂O–B₂O₃ Melts. *J. Am. Ceram. Soc.* **99**, 612–618 (2016).
31. Kirfel, A. The electron density distribution in calcium metaborate, Ca(BO₂)₂. *Act Cryst.* **B43**, 333–343 (1987).
32. Fujimoto, M. *et al.* Crystal growth and characterization of calcium metaborate scintillators. *Nucl. Instrum. Methods Phys. Res. A.* **703**, 7–10 (2013).
33. Kim, Y., Yanaba, Y. & Morita, K. Influence of structure and temperature on the thermal conductivity of molten CaO–B₂O₃. *J. Am. Ceram. Soc.* **100**, 5746–5754 (2017).

Author contributions

S.L. planned the experiments, experimental design and wrote the manuscript. X.W., X.L., G.L. and S.L. conducted the experiments.

Competing interests

The authors declare no competing interests.

Additional information

Correspondence and requests for materials should be addressed to S.L.

Reprints and permissions information is available at www.nature.com/reprints.

Publisher's note Springer Nature remains neutral with regard to jurisdictional claims in published maps and institutional affiliations.



Open Access This article is licensed under a Creative Commons Attribution 4.0 International License, which permits use, sharing, adaptation, distribution and reproduction in any medium or format, as long as you give appropriate credit to the original author(s) and the source, provide a link to the Creative Commons licence, and indicate if changes were made. The images or other third party material in this article are included in the article's Creative Commons licence, unless indicated otherwise in a credit line to the material. If material is not included in the article's Creative Commons licence and your intended use is not permitted by statutory regulation or exceeds the permitted use, you will need to obtain permission directly from the copyright holder. To view a copy of this licence, visit <http://creativecommons.org/licenses/by/4.0/>.

© The Author(s) 2020